Title
THE INTERACTIONS. OF 4-NITROQUINOLINE-1-OXIDE WITH FOUR DEOXYRIBONUCLEOTIDES

Permalink
https://escholarship.org/uc/item/2vf5591d

Author
Winkle, S.A.

Publication Date
1977-09-01

Peer reviewed

UC-4

LBL-6759
Preprint

THE INTERACTIONS OF 4-NITROQUINOLINE-1-OXIDE WITH
FOUR DEOXYRIBONUCLEOTIDES

Stephen A. Winkle and Ignacio Tinoco, Jr.

September 1977

LBL-6759

The Interactions of 4-Nitroquinoline-1-Oxide with

Four Deoxyribonucleotides[†]

Stephen A. Winkle[*] and Ignacio Tinoco, Jr.

Lawrence Berkeley Laboratory
University of California
Berkeley, California

ABSTRACT: The interactions of 4-nitroquinoline-1-oxide
(NQO) with the four 5'-deoxyribonucleotides were probed
using absorption spectra of the charge transfer bands
and ^{1}H and ^{13}C NMR spectra of nucleotide-NQO mixtures.
Applying a Benesi-Hildebrand type equation to the
spectral data yielded equilibrium constants (K(dpG:NQO) =
16 $\underline{M}^{-1}$, K(dpA:NQO) = 12 $\underline{M}^{-1}$, K(dpT:NQO) = K(dpC:NQO) =
4 $\underline{M}^{-1}$) which suggest the preference of NQO for the
guanine residue in a DNA.   From ^{13}C and ^{1}H NMR data,
a structure for the dpG:NQO complex is proposed.

The carcinogenicity and mutagenicity of substituted quinoline-1-oxides, such as 4-nitroquinoline-1-oxide[1], as well as their interaction with DNA have been demonstrated in numerous studies (Nakahara et al., 1975, Paul and Montgomery, Jr., 1970, Okano et al., 1969). Nagata and colleagues (1966), using flow dichroism techniques, showed that NQO, in its interaction with DNA, lies in plane with the DNA bases. That the presence of NQO increases the Tm's for native DNA as well as for poly(dG)·poly(dC) and to a lesser extent poly(dA)·poly(dT) was reported by Paul and Montgomery (1970).

Okano and co-workers (1969) examined the new spectral bands resulting from the formation of charge transfer complexes of NQO and deoxyribonucleosides or DNA. For the four deoxyribonucleosides, they determined equilibrium constants for the formation of 1:1 complexes:

$$NQO + dN \overset{K'}{\rightleftharpoons} NQO:dN$$
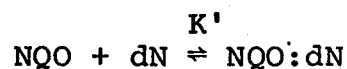
Complex band absorption vs. nucleoside concentration data (at fixed NQO concentrations) were analyzed by a

form of the Benesi-Hildebrand (Benesi and Hildebrand, 1949) equation where ℓ is the cell pathlength: A_T is the total absorbance at the complex λ_{MAX}; $[dN]_T$ and $[NQO]_T$ are the total concentrations of nucleoside and NQO; and ε is the molar absorptivity of the complex:

$$\frac{\ell[NQO]_T}{A_T} = \frac{1}{K'\varepsilon[dN]_T} + \frac{1}{\varepsilon}$$

Okano's work showed that the equilibrium constants for the complexes with the purine deoxynucleosides dG and dA [K(dG) = 12.2 $\underline{M}^{-1}$, K(dA) = 11.5 $\underline{M}^{-1}$] are larger than those for the pyrimidine compounds dT and dC [K(dT) = 5.20 $\underline{M}^{-1}$, K(dC) = 2.29 $\underline{M}^{-1}$].

Okano and co-workers (1969) also conducted a ^{1}H NMR study of mixtures of the deoxyribonucleosides and NQO. This study was done in DMSO-d6 rather than in aqueous media and was performed at high concentrations (nucleosides and NQO at $\underline{ca}$. 0.30 mole kg^{-1}).

For further insight into the base specificity of NQO binding, we have made studies of the 1:1 complexes of NQO with the 5'-deoxyribonucleotides:

$$NQO + dpN \overset{K}{\rightleftharpoons} NQO{:}dpN$$

Data from nucleotide concentration vs. complex band absorption spectra were analyzed by a Benesi-Hildebrand equation which was modified to account for nucleotide absorption and changes in the nucleotide and NQO concentrations due to complex formation. We also studied the interaction by ^{1}H and ^{13}C NMR in aqueous media and at reduced concentrations to minimize self aggregation of the nucleotide. From the magnitudes and signs of the changes in chemical shift of the protons and carbons on the molecules in the complex it was possible to propose structures for the complexes.

Materials and Methods

The four deoxyribonucleotides, dpG, dpA, dpT, dpC, were obtained from Cal Biochem. The NQO was synthesized from quinoline-1-oxide (Aldrich Chemical Company) using the procedure of Ochiai (1953), and was recrystallized three times from hot acetone.

Optical studies were done in a buffer consisting of 0.1 M NaCl and 0.01 M sodium cacodylate, pH = 7.0. Concentrations of the nucleotide and NQO solutions were measured using the absorbance at the λ_{MAX}. (See Table I

for the molar absorptivities of NQO at various wave-
lengths.) Glass tuberculin syringes were used for the
measurement of nucleotide and NQO solution volumes.
Samples for the optical studies were prepared by placing
a fixed volume of stock NQO solution in each sample
tube ($[NQO]_T$ for the samples ranged from ca.6 x 10^{-4}
to 2 x 10^{-4} M), adding a given volume of the stock
nucleotide solution ($[dpN]_T$ ranged from ca. 9 x 10^{-2} to
2 x 10^{-2} M), and then addition of sufficient cacodylate
buffer to produce constant volume. Absorption spectra
in the region of the complex band (460 - 380 nm) were
recorded for each dpN-NQO mixture vs. a solution of
equal $[NQO]_T$ to produce difference spectra. Absorption
spectra were recorded at 25°C on either a Cary 15,
Cary 14 or a Beckman Acta MIV spectrometer. For
mixtures of dpG and NQO ($[dpG]_T$ from 0.026 to 0.17 M
and $[NQO]_T$ from 4.4 x 10^{-4} to 5.5 x 10^{-4} M), absorption
spectra (460 - 380 nm) were recorded at 10°C on a Cary
14 spectrometer. Samples were run in either 0.5 or
1.0 cm pathlength cells vs. a solution of NQO alone
of equal concentration. In this manner the spectra

obtained were the difference between the sample and reference cells. The $\varepsilon_{(dpN)}$ values at the complex λ_{MAX} were obtained by measuring the absorption at these λ_{MAX} of nucleotide solutions of concentrations similar to those for the dpN-NQO mixtures. Values of $\varepsilon_{(dpN)}$ from the CRC Handbook of Biochemistry and Moleculor Biology were used at the wavelength maximum for the nucleotides to obtain the nucleotide concentrations. The $\varepsilon_{(NQO)}$ at the various complex band λ_{MAX} were similarly obtained.

Solutions for the ^{13}C NMR studies were prepared in a manner similar to that used for the optical samples. NQO was dissolved in the cacodylate buffer in H_2O and the nucleotides were dissolved in D_2O. Samples were prepared by combining 0.250 ml of the NQO solution ($[NQO]_T = \underline{ca.}$ 1 $\underline{mM}$) with a given amount of nucleotide solution ($[dpN]_T$ ranged from $\underline{ca.}$ 3 x 10^{-2} to 1.4 x 10^{-1} $\underline{M}$) and the total volume was brought up to 0.500 ml with additional D_2O. This gave a buffer concentration of 0.05 $\underline{M}$ NaCl and 0.005 $\underline{M}$ sodium cacodylate, pH = 7.0. The ^{13}C NMR spectra were obtained at 37°C (ambient temperature on this instrument) on a Nicolet TT-23 system at 25.1 MHz, using quadrature phase detection

with 8 mm sample tubes. The ^{13}C NMR spectra were referenced to dioxane (1672.0 Hz). Spectra had spectral width of 5000 Hz with 8 K data points, giving a resolution of 1.25 Hz.

The ^{1}H NMR samples were prepared by mixing 0.250 ml of the NQO solution (in cacodylate) with nucleotide (in D_2O) and D_2O to a total volume of 0.500 ml. The NQO concentration was ca. 1×10^{-3} M and $[dpN]_T$ ranged from 1×10^{-2} to 5×10^{-2} M. This mixture was lypholized and 0.500 ml D_2O used to redissolve it. The ^{1}H NMR spectra were referenced to TSP (0.00 HZ) and were run at 20°C on the Stanford Magnetic Resonance Laboratory 360 MHz system. Spectral width was 3600 Hz with 16 K data points, resolution 0.45 Hz.

Since NQO is a potent carcinogen and mutagen, all work with the solid compound, such as preparation of stock solutions, was done in a glove box. Gloves were worn when handling solutions and only small volumes of solutions were transferred outside the glove box. Glassware was washed with special care and all waste liquids and solid waste were collected for special disposal.

Results

The absorption spectra for the dpN-NQO mixtures were difference spectra obtained by subtracting the NQO absorbances. This allowed for clearer observation of the complex bands which would have otherwise appeared as shoulders on the 365 nm band of the NQO. The complex band maxima and molar absorptivities are tabulated in Table II.

In a mixture of a nucleotide and NQO, the absorbance at the complex band maximum recorded against a solution of NQO of the same initial concentration may be expressed as:

$$A_T = \ell \left(\varepsilon_c - \varepsilon_{(dpN)} - \varepsilon_{(NQO)} \right) [c] + \ell \, \varepsilon_{(dpN)} [dpN]_T$$

where A_T, $[NQO]_T$, ℓ are as defined earlier; ε_c, $\varepsilon_{(NQO)}$ and $\varepsilon_{(dpN)}$ are the molar absorptivities of the complex, NQO and the nucleotide; $[dpN]_T$ is the total nucleotide concentration and $[c]$ is the complex concentration. From this absorption expression and the equilibrium equation, a modified version of the Benesi-Hildebrand equation was derived where A_{dpN} is the absorption of the nucleotide at the complex λ_{MAX}:

$$\frac{\ell [NQO]_T}{A_T - A_{dpN}} = \frac{1}{K\left(\epsilon_c - \epsilon_{(dpN)} - \epsilon_{(NQO)}\right)} \frac{1}{[dpN]_T} + \frac{1}{\epsilon_c - \epsilon_{(dpN)} - \epsilon_{(NQO)}}$$

This equation was derived with the assumption that

$[dpN]_T \gg c$ so that $[dpN] = ([dpN]_T - [c]) \cong [dpN]_T$ where $[dpN]$

is the equilibrium concentration. To help maintain

this assumption, $[dpN]_T$ was always much larger than

$[NQO]_T$. The quantity, A_{dpN}, was calculated using $[dpN]_T$

and $\epsilon_{(dpN)}'$ – based on the assumption that the amount of

complex was much less than $[dpN]_T$. Since nucleotides

do not absorb at $\lambda \cong 400$ nm, the absorbances (which are

linear with $[dpN]$) observed for the nucleotides at such

wavelengths are probably due to the small amounts of

impurities which become observable at the high nucleotide

concentrations employed. By plotting the term,

$\ell [NQO]_T / (A_T - A_{dpN})$, against $1/[dpN]_T$, the equilibrium

constants for complex formation were obtained. Figures

1(a)-1(d) give the plots and least squares fits of the

data from the studies at room temperature of the complex

absorption bands for the four dpN:NQO complexes. The

equilibrium constants of complex formation obtained

from these plots are summarized in Table II.

To assay the temperature dependence of the dpG-NQO equilibrium, an optical study of dpG-NQO mixtures was made at 10°C as well as 25°C. The Benesi-Hildebrand type plot is shown in Figure 1(e). The equilibrium constant at 10°C was determined to be 23 $\underline{M}^{-1}$. From the van't Hoff equation, values of $\Delta H° = - 4.2$ kcal-mole^{-1} and $\Delta S° = - 8.5$ cal-mole^{-1}-deg^{-1} were calculated. Using these quantities, the equilibrium constants at other temperatures for the dpG-NQO system could be calculated, e.g., $K(20°C) = 18 \underline{M}^{-1}$.

Because of the low solubility of NQO in aqueous media (<u>ca</u>. 2 - 3 <u>mM</u>), the ^{13}C NMR spectrum of NQO could not be obtained in a reasonable period of time with the present equipment. Thus, the ^{13}C NMR spectra of dpN-NQO mixtures gave only the spectra of the nucleotide. The observed chemical shifts were the weight averages of the free and bound chemical shifts of the nucleotide carbons.

In Figure 2, the differences between δ_{OBS} for dpG base carbons in the dpG:NQO mixtures and δ_{FREE} for those carbons (at the same dpG concentrations as in each mixture) are plotted <u>vs</u>. the dpG/NQO ratio. Carbon-8

of the base shows a large downfield shift (to lower
field strength) with a decreasing dpG/NQO ratio (and
hence, increasing fraction of bound dpG). The maximum
amount of dpG in the complex in these mixtures was
approximately 1%. For a sample with 1% of the dpG
complexed, a shift change for C-8 of ca. 0.4 ppm is
observed. Carbon-6, the carbonyl carbon, shows a
lesser, but still fairly large downfield shift. The
other observable base carbons (all except C-4) show
much smaller downfield shift changes. The only sugar
carbon of dpG to show any shift change was C-2'.

Carbons C-2, C-8, C-4 and C-6 are the only readily
observable base carbons of dpA. The relaxation time
(T_1) of C-5 and the broadening of this carbon's signal
due to complexation inhibit its observation. The
chemical shift changes for the dpA carbons observed
in a concentration range similar to that of the dpG-
NQO systems are all small downfield shifts. None of
the carbons give large shift changes as were observed
with C-8 and to a lesser extent C-6 of dpG.

The ^{13}C NMR spectra of dpT-NQO mixtures were
measured. No apparent changes due to complexation
in any of the dpT carbon chemical shifts were observed.

The chemical shifts of the protons of NQO when complexed with dpG or dpA were calculated from the following relation, where δ_B, δ_{OBS}, δ_{FREE} are the chemical shifts of a proton in the bound state, in the NQO-dpN mixture and free NQO solution, respectively:

$$\delta_B = \left(\delta_{OBS} - \delta_{FREE}\left(\frac{[NQO]_T - [c]}{[NQO]_T}\right)\right)\frac{[NQO]_T}{[c]}$$

The δ_B and the difference between δ_B and δ_{FREE} for the NQO protons were calculated using the δ_{OBS} from the ^{1}H NMR spectra of dpN-NQO mixtures. For the dpG-NQO mixtures the equilibrium constant at 20°C (the temperature of the ^{1}H spectra) was calculated to be 18 $\underline{M}^{-1}$ from the optical measurements at 10°C and 25°C. Having this equilibrium constant enabled us to calculate the complex concentrations for the dpG-NQO mixtures and thus δ_B. For the dpA-NQO mixtures, the [c] at 20°C were estimated using the equilibrium constant at 25°C. The values of δ_B were then calculated using these [c]'s.

In Table III, the calculated δ_B and $|\Delta(\delta_B - \delta_{FREE})|$ for the NQO protons are presented for dpG-NQO and dpA-NQO mixtures.
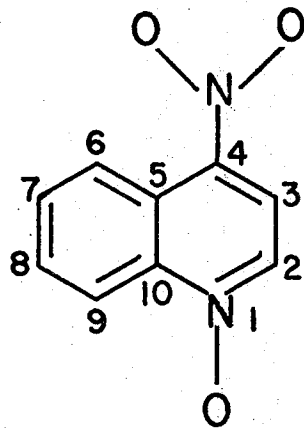
For NQO complexed with both dpG and dpA, H-6 and H-9
show the largest changes in chemical shift. For NQO
in the dpG-NQO mixtures, H-2 and H-3 are the next
largest. However, for NQO in dpA-NQO solutions, H-7
and H-8 show the next largest changes after H-6 and
H-9. All shifts are upfield, to higher field strength.

Discussion

Optical Studies of the Charge Transfer Bands.
The complexes of the four deoxynucleotides with NQO have
similar molar absorptivities and the λ_{MAX} for the four
are likewise at about the same wavelength (of about
equal energy). The molar absorptivities were obtained
from the Benesi-Hildebrand type plots. The form of
the Benesi-Hildebrand equation used differed from that
of Okano through the inclusion of terms for changes in
nucleotide and NQO concentration due to complex forma-

tion. The ε_c given in Table II differ from those obtained by Okano although the reciprocals of our intercepts $\frac{1}{(\varepsilon_c - \varepsilon(dpN) - \varepsilon(NQO))}$ are similar to Okano's values of ε_c.

That the data for all four mononucleotides gave linear Benesi-Hildebrand type plots indicates that the four mononucleotides form 1:1 complexes with NQO. The preference of NQO for the purine nucleotides is indicated by the larger magnitude of the equilibrium constants for the purines vs. the pyrimidine systems as found earlier by Okano for the nucleosides. The equilibrium constants for the nucleotide systems are also similar to those obtained by Okano for the nucleosides. For example, the equilibrium constant for the dpG-NQO system is 16 $\underline{M}^{-1}$ vs. 12.2 $\underline{M}^{-1}$ for the dG-NQO system. This suggests that the addition (in the 5' position) of a phosphate group to the deoxyribose does not alter to any large extent the binding of NQO to the base portion of the nucleotide.

NMR Studies of the dpG Mixtures and dpG:NQO Complex Structure. As is shown in Figure 2, all dpG base carbon chemical shifts move downfield in the presence of NQO.

The proton chemical shift changes for the NQO protons
are upfield. This results from the ring current
effect of the dpG base on the NQO protons when NQO is
stacked with the dpG base. Since the NQO is stacked
with the dpG base, the downfield ^{13}C NMR shift changes
cannot be due to the dpG base and NQO being in the
same plane. The downfield direction of the shift
differences could be due to the change in electron
density in the base in the charge transfer complex
with NQO. Since dpG acts as the electron donor in the
complex, its electron density would be diminished
somewhat leading to an increase in the magnitude of the
paramagnetic shielding term (Karplus and Pople, 1963;
Cheney and Grant, 1967) and hence, a downfield shift
change. One would expect a corresponding upfield
shift change for NQO carbons. The larger shift
difference of C-8 relative to the other base carbons
suggests that the imidazole ring of the base is stacked
with the electron-withdrawing portion of the NQO, i.e.,
the nitro and oxide containing ring. The somewhat
smaller shift change for C-6 implies that there is also
some electron withdrawal through the carbonyl group.

As stated, the shift changes for the NQO protons
are all upfield as would be expected if the ring
current of the complexed dpG base dominates the complex
effects. However, the shifts are much smaller than
those observed for interactions in which aromatic
molecules stack without charge transfer, e.g., nucleic
acid base stacking (Schweizer, et al. 1968) and ethidium
bromide-nucleic acid interactions (Che-Hung Lee,
personal communication). The charge transfer inter-
action may somewhat negate the upfield shift due to
the ring current of the base. The amount of electron
transfer is too small, though, to alter to any major
degree the magnitude or shape of the ring current. Hanna
and Ashbaugh (1964) observed such a negation of the
ring current effect for various charge transfer systems.
In any case, if the assumption is made that the center
of the ring current is essentially where Giessner-
Prettre and Pullman (1970, 1976) place it, i.e., in
the imidazole ring beside the center of the C-4 - C-5
bond, the shifts in Table III may be used to help
orient the molecules in the complex.

Protons H-6 and H-9 of the NQO show the largest shift and are placed near the C-4 - C-5 bond of the base. The ^{13}C NMR data suggests that the nitro and oxide containing ring is stacked with the imidazole base ring so H-2 and H-3 must be placed over that ring and H-7 and H-8 over the other. Additionally, the proton shift changes rule out the placement of the benzene-like ring of NQO with the imidazole ring. After the manipulation of models to arrive at the best fit of proton chemical shift changes, the orientation in Figure 3 was determined for the dpG:NQO complex. The structure places the positive center of the oxide region of NQO near the electron-rich N-9 of dpG and the electron-attracting region of the NQO nitro group near the carbonyl of dpG. Both areas on dpG contain carbons (C-8 and C-6) showing the largest ^{13}C NMR shift changes.

NMR Studies of the dpA-NQO Mixtures. In the ^{13}C NMR spectra of the dpA in dpA-NQO mixtures, no carbons on the dpA base show the large downfield shift of C-8

of dpG. Indeed, no dpA carbons show different enough
chemical shift changes which might distinguish the
position in the complex of one region of the dpA base
relative to another. This lack of distinguishability
and the small size of all the shifts could imply that
no single isolated region of the dpA, such as the
imidazole ring and C-8, is the center of electron
withdrawal. The equilibrium constant for dpA:NQO
formation is not sufficiently smaller than that of
dpG:NQO formation to account for the smaller values
of $|\Delta(\delta_{OBS}-\delta_{FREE})|$ in the dpA-NQO mixtures.

The proton chemical shift differences for NQO
protons in dpA-NQO mixtures, presented in Table III,
are larger than those for dpG-NQO mixtures. This is
expected since the ring current of dpA is larger than
that of dpG. Whereas for dpG:NQO, the chemical shifts
of NQO H-7 and H-8 are apparently unchanged by
complexation, for dpA:NQO these protons show the next
largest $|\Delta(\delta_{OBS}-\delta_{FREE})|$ after H-6 and H-9. As in
dpG:NQO, the shift changes of H-6 and H-9 for dpA:NQO
are the greatest, suggesting that these protons are
the closest to the ring current center of dpA. Protons

H-2 and H-3 have the smallest shifts and therefore are the farthest from the ring current center.

The lack of a large shift difference for the imidazole ring C-8 implies that the electron withdrawing ring of NQO is not placed solely over this ring. If this is the case, then the possible orientation of dpA:NQO which gives the best fit to the Giessner-Prettre and Pullman (1976) ring current model of dpA is roughly the reverse of that of dpG:NQO. The benzene-like ring of NQO is over the imidazole ring and the nitro and oxide ring is over the pyrimidine ring. Without the detailed ^{13}C NMR information obtainable for dpG-NQO mixtures, arriving at a more precise picture is difficult.

NMR Studies with dpT. As was stated earlier, no ^{13}C chemical shift changes were observed for mixtures of dpT and NQO. This is probably due to the small equilibrium constant for complex formation. For this reason ^{1}H NMR studies with dpT and ^{1}H and ^{13}C NMR studies with dpC were not attempted.

Conclusions

Using Benesi-Hildebrand type plots, the equilibrium
constants for the formation of 1:1 complexes of dpG, dpA,
dpT and dpC with NQO were obtained. These equilibrium
constants, which are similar in value to those obtained
for the deoxynucleosides, indicate the preference of
NQO for the guanine residues of DNA, a conclusion which
the deoxynucleoside studies also suggested. From ^{13}C
and ^{1}H NMR studies, an orientation for the dpG:NQO
complex was obtained and insight into the dpA:NQO complex
orientation was gained.

NQO, rather than a possible metabolite such as
4-hydroxyaminoquinoline-1-oxide, could possibly be the
species which interacts with the bases of DNA. An
electron spin resonance study by Okano and Uekama on
NQO free radicals showed that DNA enhanced the formation
of NQO free radicals - which might suggest that DNA
helps metabolize the NQO to an adduct forming species
(Okano & Uekama, 1968). Knowledge of the structure
of the non-covalent complexes of NQO and the DNA bases
(as in nucleotides or dinucleosides) should provide informa-
tion on the formation of and the structure of adducts.

Our studies indicate that the use of NMR and optical methods for studying complexing of NQO with dinucleotides is feasible. Such a study, which should yield information about sequence specificity and give a better picture of NQO orientation in DNA, is now underway.

References

Benesi, H. A. and Hildebrand, J. H. (1949), *J. Am. Chem. Soc. 71*, 2703.

Cheney, B. V. and Grant, D. M. (1967), *J. Am. Chem. Soc. 89*, 3319.

Giessner-Prettre, C. and Pullman, B. (1970), *J. Theor. Biol. 27*, 87.

Giessner-Prettre, C. and Pullman, B. (1976), *Biochem. Biophys. Res. Comm. 70*, 578.

Hanna, M. W. and Ashbaugh, A. L. (1964), *J. Phys. Chem. 68*, 811.

Karplus, M. and Pople, J. A. (1963), *J. Chem. Phys. 38*, 2803.

McCann, J., Choi, E. Yamasaki, E. and Ames, B. N. (1975) *Proc. Nat. Acad. Sci. USA 72*, 5135.

Nagata, C., Kodama, M., Tagashira, Y. and Imamura, A.
(1966), *Biopolymers 4*, 409.

Nakahara, W., Fukuoka, F. and Sugimura, T. (1957),
Gann 48, 129.

Okano, T., Niitsuma, A., Takadata, A. and Uekama, K.
(1969), *Gann 60*, 97.

Okano, T., Uekama, K. and Taguchi, E. (1969), *Gann 60*,
295.

Okano, T., Takadata, A. and Kano, T. (1969), *Gann 60*,
557.

Okano, T. and Uekama, K. (1968), *Chem. Pharm. Bull.*
(Tokyo) *16*, 1411.

Paul, J. S. and Montgomery, P. O'B. (1970), *Mol.*
Pharmacol. 6, 315.

TABLE I: Values of the molar absorptivity (ε) at various wavelengths for NQO (at pH = 7.0, aqueous media).

Molecule	Wavelength (nm)	Molar Absorptivity x 10^3 (M-1 cm-1)
NQO	250 (λ_{MAX})	16.5[a]
	365 (λ_{MAX})	8.40[a]
	398	3.79[b]
	402.5	3.23[b]
	405	2.69[b]
	406	2.59[b]

[a]T. Okano et al., Gann 64, 227 (1973)

[b]Experimentally determined at the wavelength maxima of the complexes (see Table II).

TABLE II: Equilibrium constants (K (25°C)) for the formation of dpN:NQO complexes

Complex	λ_{MAX}(nm)	$\epsilon \times 10^3$ $(M^{-1}\ cm^{-1})$	K(25C) (M^{-1})
dpG:NQO	406	3.3	16 ± 2
dpA:NQO	405	3.8	12 ± 2
dpT:NQO	402.5	4.0	4 ± 3
dpC:NQO	398	4.5	4 ± 3

TABLE III: Effects of nucleotide complex formation at 20°C upon NQO protons

NQO Proton	δ_{FREE} (ppm)	dpG:NQO		dpA:NQO	
		δ_B (ppm)	$\|\delta_B - \delta_{FREE}\|$ (ppm)	δ_B (ppm)	$\|\delta_B - \delta_{FREE}\|$ (ppm)
2	8.837	8.728	0.11	8.534	0.30
5	8.730	8.546	0.18	8.146	0.58
8	8.678	8.504	0.17	8.106	0.57
3	8.373	8.310	0.06	8.101	0.27
6	8.084	~8.084	~0.00	7.704	0.38
7	8.029	~8.029	~0.00	7.611	0.42

FOOTNOTES

[†]From the Department of Chemistry and Chemical
Biodynamics Laboratory, University of California,
Berkeley, CA 94720. This work was supported in
part by National Institutes of Health Grant
GM10840 and by the Division of Biomedical and
Environmental Research of the United States Energy
Research and Development Administration.

[1]Abbreviations used in this paper: 4-nitroquinoline-1-
oxide (NQO); deoxynucleosides (dN), e.g., deoxyguanosine
(dG); deoxynucleotides (dpN), e.g., deoxyguanosine-5'-monophosphate
(dpG); nuclear magnetic resonance (NMR);
3-(trimethylsilyl)-propanesulfonic acid (TSP);
dimethyl sulfoxide-d_6 (DMSO-d_6).

FIGURE CAPTIONS

Figures 1(a-e): Benesi-Hildebrand-type plots
of NQO-dpN complex spectral data. Temperatures:
1(a-d), 25°C, 1(e) 10°C. Buffer: Na cacodylate
0.01 $\underline{M}$, NaCl 0.1 $\underline{M}$, pH = 7.0. Concentrations:
$[dpN]_T$ 1.7 x 10^{-1} - 2 x 10^{-2} $\underline{M}$, $[NQO]_T$ 6 x 10^{-4} -
2 x 10^{-4} $\underline{M}$.

Figure 2: ^{13}C NMR chemical shift data for
dpG/NQO mixtures. All shifts are downfield.
Temperature: 37°C. Solvent: Na cacodylate
0.005 $\underline{M}$, NaCl 0.05 $\underline{M}$, $D_2O:H_2O$ (1:1), pH = 7.0.
Concentrations: $[dpN]_T$ 3 x 10^{-2} - 1.4 x 10^{-1} $\underline{M}$,
$[NQO]_T$ $\underline{ca}$. 1 mM. 5000 Hz spectral width, 8 K
data points.

Figure 3: Proposed structure of dpG/NQO complex.
NQO (●-●) is in a plane parallel to guanine (o-o)
and about 3.4Å above it.
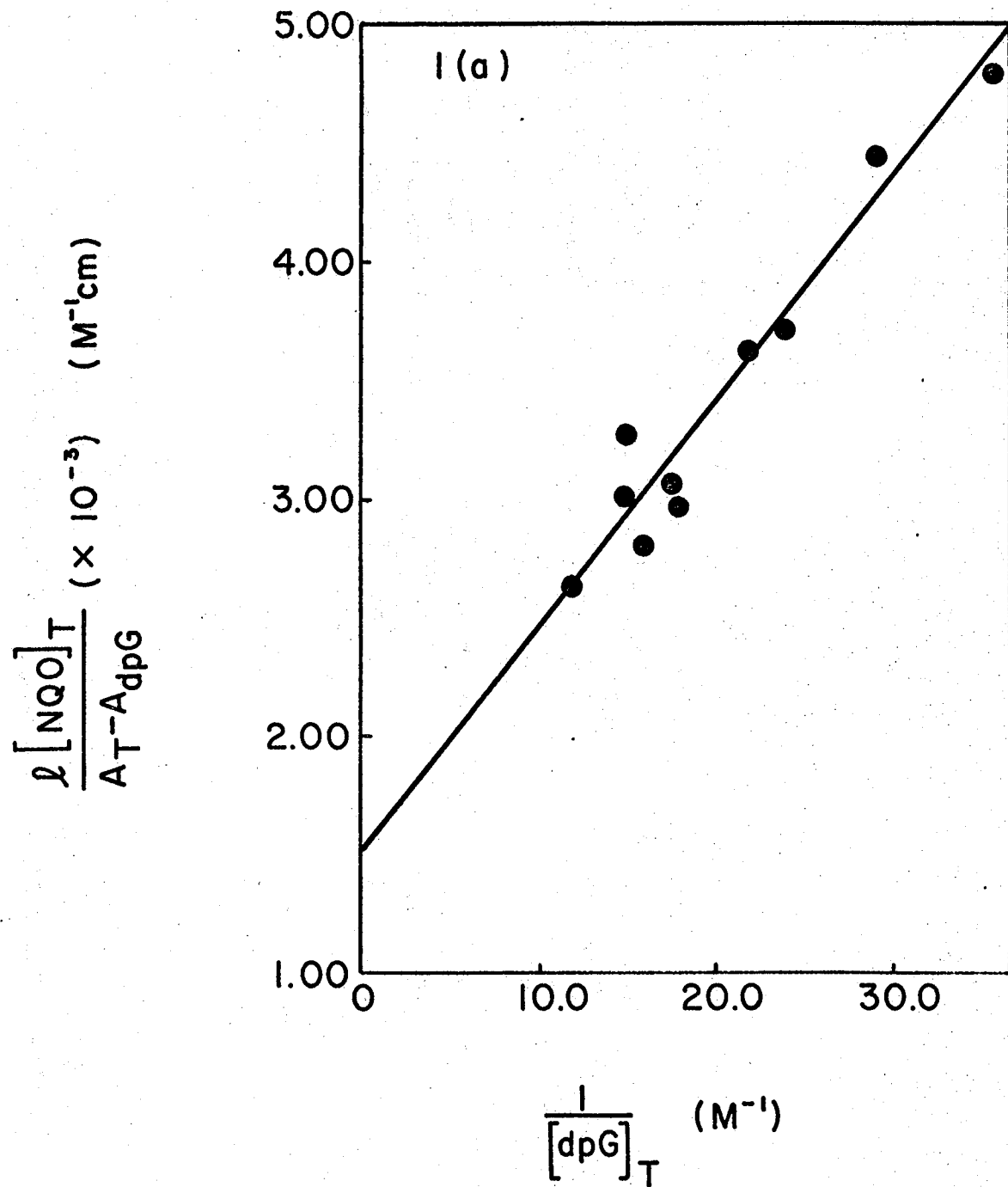
Figure 1(a)

XBL 778-2987
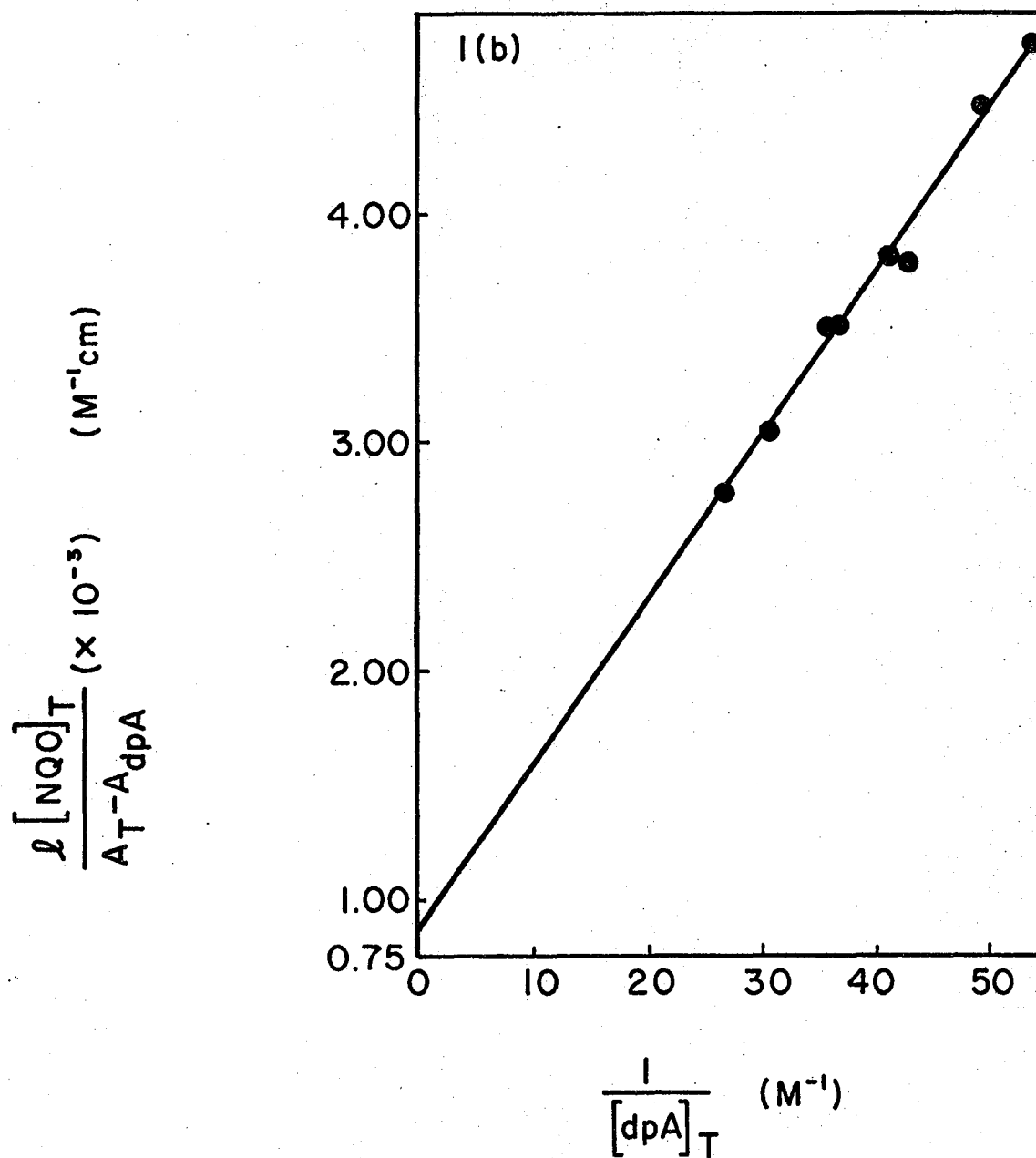
Figure 1(b)
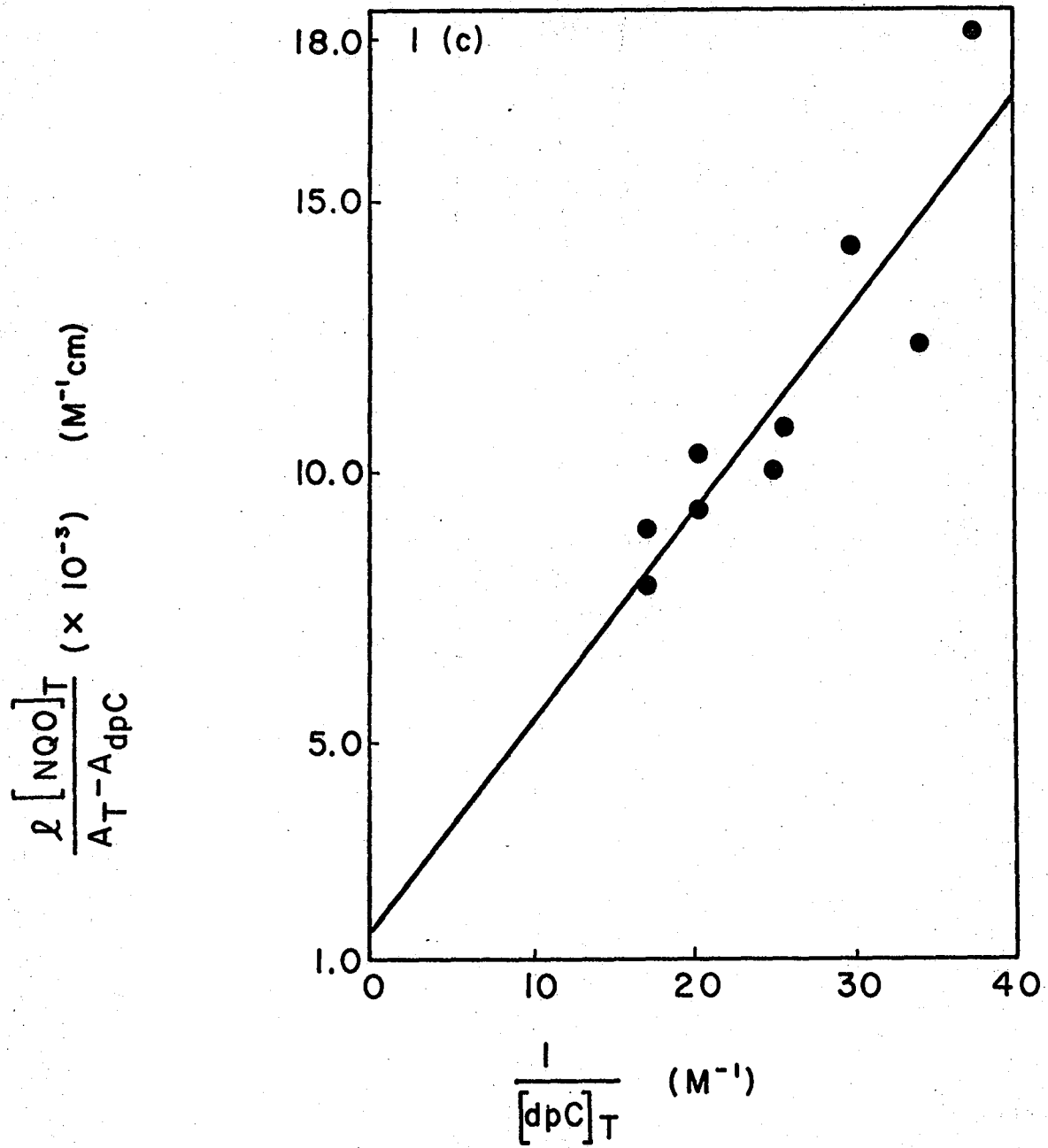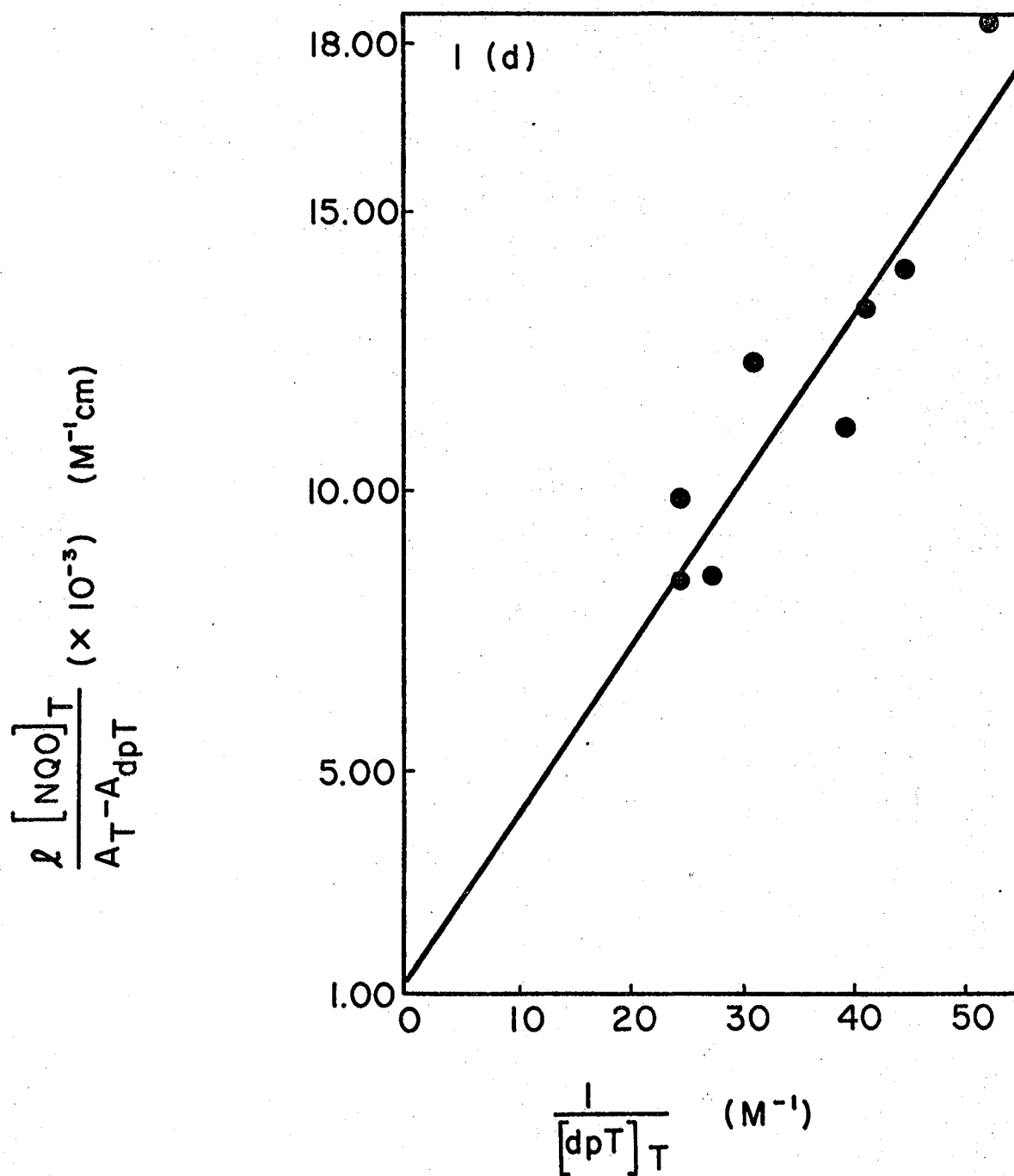
Figure 1(c)

Figure 1(d)

XBL 778-2985
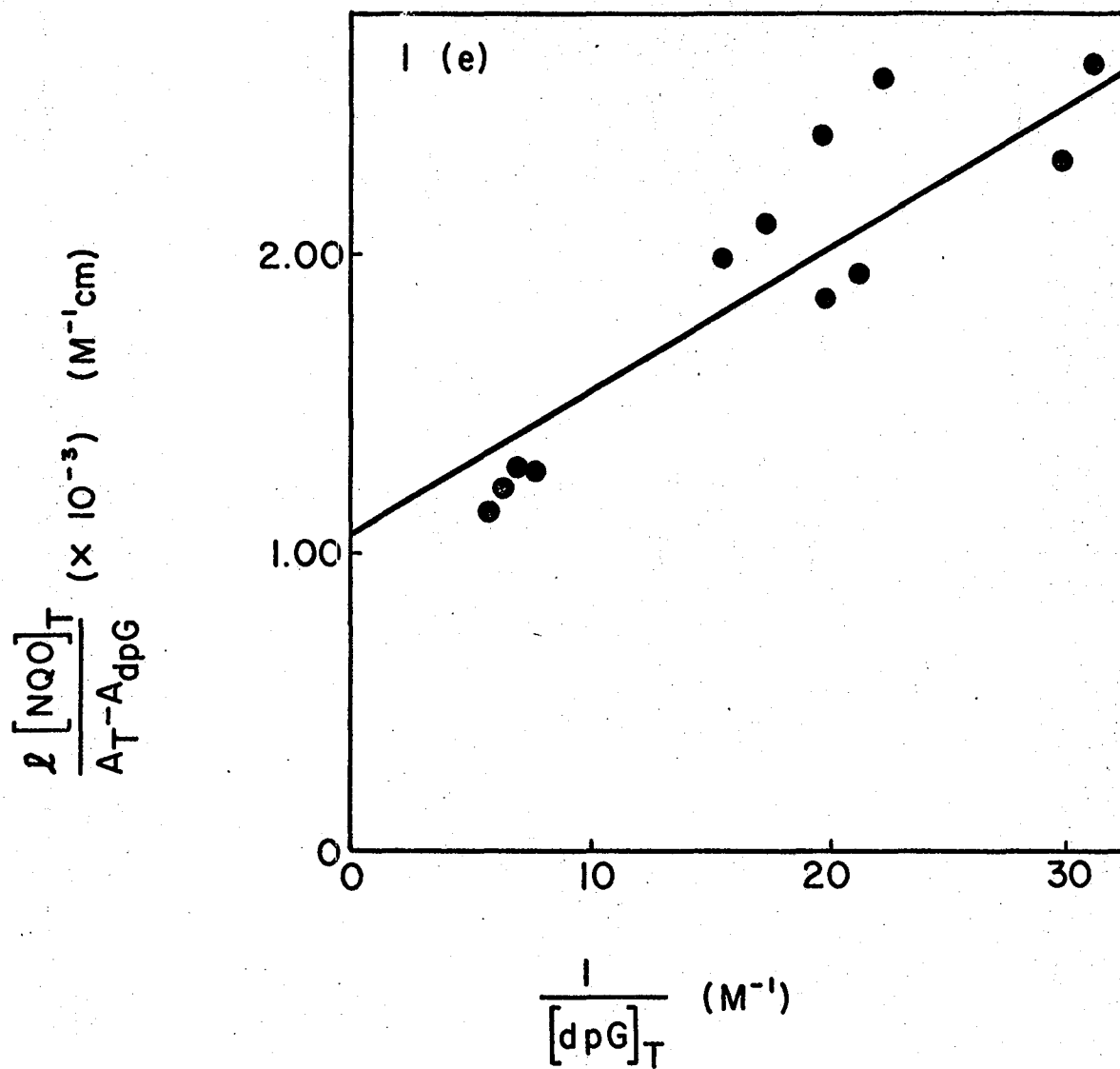
Figure 1(e)

XBL 778-2982

Figure 2

XBL 778-2988

Figure 3